Probing extradiol dioxygenase mechanism in NAD^+ biosynthesis by viewing reaction cycle intermediates

Ian Davis and Aimin Liu

Department of Chemistry, University of Texas, San Antonio, TX, USA

FUNCTIONAL CLASS

Enzyme; EC 1.13.11.6; type III extradiol dioxygenase; 3-hydroxyanthranilate 3,4-dioxygenase, known as HAO, HAD, and HAAO.

HAO catalyzes the activation and insertion of molecular oxygen into 3-hydroxyanthranilic acid (3-HAA), a metabolite of tryptophan degradation, to generate 2-amino-3-carboxymuconate-6-semialdehyde (ACMS), an unstable metabolite that can nonenzymatically cyclize to form quinolinic acid (QUIN) as shown in Figure 1.[2,3]

OCCURRENCE

HAO was first discovered as a component of the kynurenine pathway, which is responsible for the majority of tryptophan catabolism in mammals.[4–7] The kynurenine pathway has also been found in some bacteria.[8,9] Additionally, HAO is found in a bacterial 2-nitrobenzoate catabolic pathway that allows the bacteria to survive using 2-nitrobenzoate as their sole source of carbon, nitrogen, and energy.[10,11]

BIOLOGICAL FUNCTION

The primary function of HAO is to break the stable phenyl ring of the substrate oxidatively. Its immediate product ACMS either nonenzymatically decays to QUIN[12] or is decarboxylated by an enzyme known as ACMSD.[13] QUIN is the universal precursor for the biosynthesis of the nicotinamide ring of NAD(P).[14] However, elevated levels of QUIN are associated with neurodegenerative diseases due to its ability to aberrantly agonize *N*-methyl-D-aspartate (NMDA) receptors.[15,16] As such, the kynurenine pathway and HAO have been recognized as potential targets for drug development.[17,18] Alternatively, ACMS can be enzymatically processed via the glutarate pathway of tryptophan

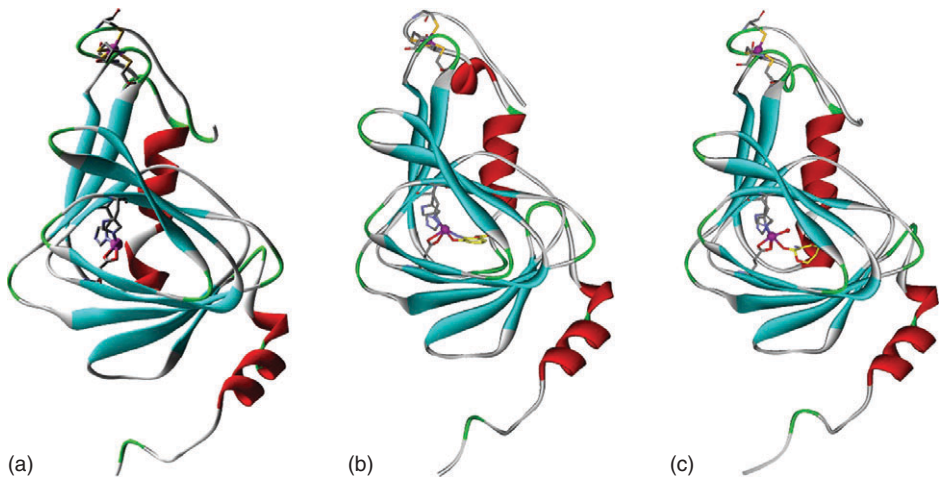

3D Structure Ribbon representations of 3-hydroxyanthranilate 3,4-dioxygenase (HAO) in the (a) ligand free form (PDB code: 6VI5), (b) substrate-bound (PDB code: 6VI7), and (c) monooxygenated seven-membered lactone intermediate (PDB code: 6VIA). The iron ions are shown in magenta balls. [These structures were prepared using Accelrys Discovery Studio Visualizer.[1]]

This article was published in the *Encyclopedia of Inorganic and Bioinorganic Chemistry* in 2022 by John Wiley & Sons, Ltd.
DOI: 10.1002/9781119951438.eibc2813

Table 1 The bond length (Å) of the endogenous ligands to the catalytic iron ion

	Substrate-free (PDB code: 6VI5)	Superoxo (PDB code: 6VI8)	Alkylperoxo (PDB code: 6VI9)	Lactone (PDB code: 6VIA)	$(ACMS)_I$ (PDB code: 6X11)	$(ACMS)_{I,II}$ (PDB code: 6VIB)
His51 (N_δ)	2.2	2.2	2.5	2.2	2.3	2.3
His95 (N_ε)	2.2	2.1	2.4	2.1	2.3	2.2
Glu57 (carboxylate)	2.3, 2.6	2.3, 2.6	2.4, 2.6	2.1, 2.3	2.4, 2.5	2.3, 2.4

$(ACMS)_I$ and $(ACMS)_{I,II}$ correspond to two conformations of the dioxygenation products bound to the catalytic iron ion, respectively.

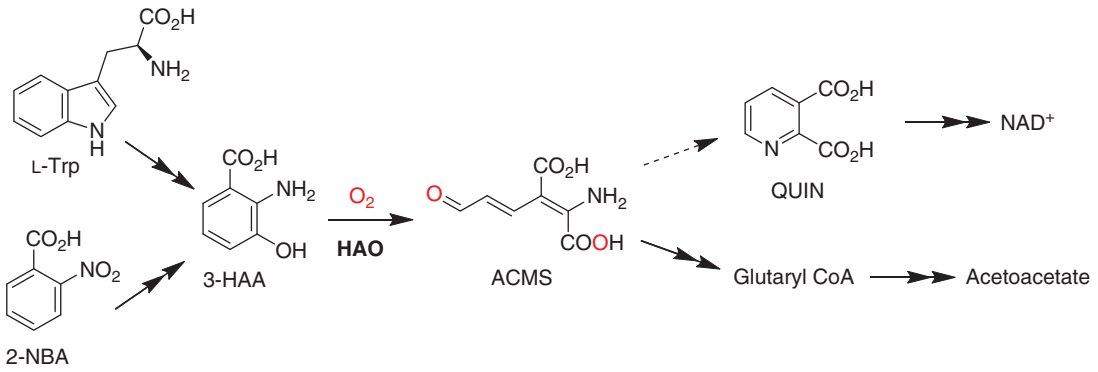

Figure 1 HAO is found in the catabolic pathways for tryptophan and 2-nitrobenzoic acid, generating QUIN as a precursor for NAD(P) biosynthesis or allowing for complete oxidation via the citric acid cycle. Solid arrows represent enzymatic transformations, and dashed arrow represents spontaneous electrocyclization. [Adapted from Mehler[2]; Colabroy and Begley.[3]]

metabolism to α-ketoadipic acid, which can be further metabolized to glutaryl-CoA and acetyl-CoA, ultimately being fully oxidized to CO_2.[19] In bacteria capable of catabolizing 2-nitrobenzoate, HAO catalyzes the most chemically challenging step, breaking the aromatic ring, so that ammonia can be released and energy can be harvested by the citric acid cycle via acetyl CoA.[11]

AMINO ACID SEQUENCE INFORMATION

HAOs from unicellular and multicellular sources differ in the length of their polypeptide chains with the former and latter being composed of roughly 170 and 280 amino acids (AA), respectively.[20] In animals, HAO is encoded by the *HAAO* gene.[21] Over 500 sequences have been identified in bacteria and fungi with many verified at the protein level.[20] HAOs are found in metabolic pathways for tryptophan[8,9] and 2-nitrobenzoic acid catabolism.[11]

- *Homo sapiens*; PDB codes: 2QNK, 5TK5, 5TKQ; HAAO (Uniprot: P46952); 286 AA
- *Bos taurus*; PDB code: 3FE5; HAAO (Q0VCA8); 286 AA
- *Saccharomyces cerevisiae*; PDB code: 1ZVF; HAAO (P47096); 177 AA
- *Cupriavidus metallidurans*; PDB codes: 1YFU, 4L2N, 4R52; 6VI5;
- *Pseudomonas fluorescens* strain KU-7 NbaC (Q1LCS4); 174 AA

PROTEIN PRODUCTION, PURIFICATION, AND MOLECULAR CHARACTERIZATION

HAO can be isolated and purified to homogeneity from beef kidney or liver for study.[22,23] Alternatively, HAO from various sources was readily cloned, overexpressed in bacteria, and purified by standard chromatographic techniques.[8,9,11]

HAOs from bacteria show marked differences from their animal counterparts. Bacterial HAOs comprise around 170 AA, have two metal-binding sites (see 3D Structure), and form dimers as their functional unit. In contrast, HAOs in animals are nearly twice as long, with more than 280 AA, and contain only one metal-binding site.[20]

ACTIVITY AND INHIBITION TESTS

HAO activity requires a ferrous ion at the active site and molecular oxygen as a co-substrate. Dioxygenation of

This article was published in the *Encyclopedia of Inorganic and Bioinorganic Chemistry* in 2022 by John Wiley & Sons, Ltd.
DOI: 10.1002/9781119951438.eibc2813

3-HAA to ACMS can be monitored spectrophotometrically by measuring increasing absorbance at 360 nm, which corresponds to the absorbance maximum of ACMS with an extinction coefficient of $\varepsilon_{360\,nm} = 47\,500\,M^{-1}\,cm^{-1}$.[24] A Clark-type oxygen electrode can also be used to measure reaction rate of HAO and its use allows for the determination of the K_M for O_2.[25]

HAO from beef kidney exhibits rapid inactivation during catalytic turnover.[22] The mechanism of inactivation is unknown, but it is a first-order kinetic process related to substrate concentration. HAO is irreversibly inhibited by 4-chloro-3-hydroxyanthranilic acid, a metabolite of 6-chlorotryptophan, as well as 4-bromo and 4-fluoro derivatives.[26–30] The inhibition was found to be due to the generation of superoxide from molecular oxygen upon forming a ternary complex that is not competent for catalytic turnover.[31] 6-chloro-3-hydroxyanthranilic acid also irreversibly inhibits HAO, though it is far less effective.[23] The activity of HAO can also be inhibited by the kynurenine pathway side product and metal chelator, picolinic acid (PIC), which can extract the active site iron ion.[20]

X-RAY CRYSTAL STRUCTURE

The first structure of HAO was solved from a bacterial source, *Ralstonia metallidurans,* which was later renamed *Cupriavidus metallidurans*, at a resolution of 1.9 Å. The bacterial enzyme has a cupin barrel fold, forms homodimers, and possesses two metal-binding sites, the catalytic site and an accessory, rubredoxin-like site.[24] A nickel-bound, eukaryotic HAO structure was solved from *S. cerevisiae* at 2.4 Å.[32] Overall, the yeast and bacterial enzymes have quite similar structures. The structure of human HAO with nickel bound at the active site was deposited in the protein data bank in 2007 by the Center for Eukaryotic Structural Genomics at a resolution of 1.6 Å (PDB code: 2QNK, no associated publication). The structure of HAO purified from the bovine kidney was solved to 2.5 Å resolution, and the two enzymes show nearly identical structures with a root mean square deviation (r.m.s.d.) of 1.2 Å over all Cα carbons.[33] Later, the structure of human HAO was solved with iron and zinc, respectively, at the active site.[34] The mammalian enzymes are comprised of two cupin domains, one which is nearly identical to the bacterial and yeast monomers and another that superposes well with a portion of the corresponding dimer. A superposition of mammalian and bacterial enzymes can be found in Figure 2. As such, the mammalian enzymes may have arisen from gene duplication, fusion, and truncation. The mammalian enzymes also lack the rubredoxin-like binding site found in HAOs from lower organisms and only binds one metal ion per functional unit as contrasted with the four of bacteria and yeast (two iron ions per monomer).

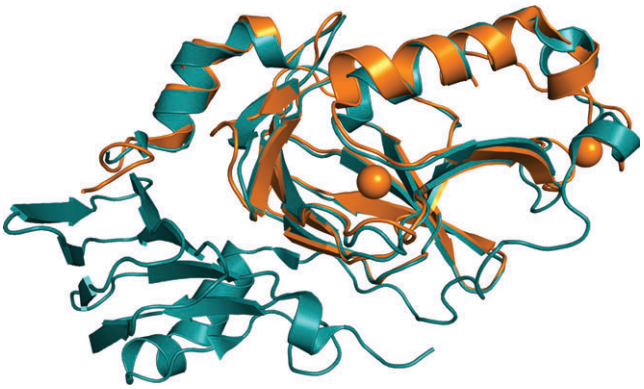

Figure 2 Superposition of human HAO (cyan, PDB code: 5TK5) and a bacterial HAO (orange, PDB code: 4R52) crystal structures.

COMPLEX STRUCTURES

To date, complex structures (binary and ternary) have only been solved for HAO from bacterial sources. The active site ferrous ion in HAO is typically coordinated by two histidines, a bidentate glutamate, and two water molecules; however, bovine HAO has only one water molecule bound to the active site iron. The substrate, 3-HAA, binds the active site ferrous ion as a bidentate ligand (PDB: 6VI7 and 1YFY), displacing the water molecules and leaving an open coordination site for oxygen binding.[24,35] Substrate binding also induces a structural rearrangement, bringing three hydrophobic loops closer to the iron center to assist binding of the hydrophobic dioxygen molecule, discussed below in the section titled on 'Functional Aspects'.[25] An intermediate, monodentate ES complex (PDB code: 6VI6) was also captured before loop movement took place.[35] Structures of additional catalytic intermediates are discussed below in the section titled on 'Catalytic Mechanism.'

Structures of HAO bound with 4-Cl-3-HAA have also been solved as ternary complex mimics with O_2 (PDB code: 1YFW), NO (PDB code: 1YFX), and in two variants designed to investigate oxygen binding (PDB codes: 6BVQ and 6BVS).[24,25] In all cases, 4-Cl-3-HAA binds with its hydroxyl group as a monodentate ligand to the active site iron. The structure of HAO bound with another inhibitor, PIC, has also been solved (PDB code: 4HSJ).[20] PIC binds the iron ion as a bidentate ligand with one oxygen of its carboxylate moiety and the nitrogen of its pyridine ring.

FUNCTIONAL ASPECTS

An accessory binding site

All HAOs have a mononuclear ferrous center at their active site coordinated by two histidines and one glutamate that is responsible for binding both substrates, 3-HAA and O_2,

This article was published in the *Encyclopedia of Inorganic and Bioinorganic Chemistry* in 2022 by John Wiley & Sons, Ltd.
DOI: 10.1002/9781119951438.eibc2813

and catalyzing dioxygenation. HAOs from unicellular organisms also contain a secondary rubredoxin-like site that coordinates a ferrous ion with four cysteines in a tetrahedral geometry. The lack of this site in higher organisms suggests that it is not essential for catalysis. The cysteine ligands were found to form disulfide bonds when superoxide is released from the active site during uncoupled oxygen activation caused by 4-Cl-3-HAA, and the process could be reversed with the addition of dithiothreitol and Fe(II).[31] The finding that the rubredoxin site can absorb oxidizing equivalents raises the question, why is it only present in unicellular organisms? One possible reason for the discrepancy between uni- and multicellular organisms is that the pathway containing HAO may be essential in lower organisms, especially those surviving on nitrobenzoate as their sole source of carbon, nitrogen, and energy. Under those conditions, the activity of HAO is a necessary, life-sustaining process, and the rubredoxin-like site might serve as a 'spare tire' carrying a backup iron ion to replenish the active site if it were to lose its iron to metal chelators. This possibility was investigated using metal reconstitution followed by Mössbauer and electron paramagnetic resonance (EPR) spectroscopies, metal analysis, activity assays, structure determination, and computational approaches.[20] ApoHAO (metal-free) was reconstituted with 1 and 2 equiv of Fe(II), or Cu(II), respectively, as well as mixed metallated HAO with Fe(II) and Cu(II) being added sequentially in either order, respectively. HAO reconstituted with a single Fe(II) exhibited more than 80% activity as compared to fully-loaded HAO, which suggests that the rubredoxin-like site is not required for activity. Mössbauer and EPR spectroscopies were used to show that the first metal presented to apoHAO preferentially binds to the active site. The X-ray crystal structures of Fe/Fe-HAO (PDB code: 4L2N), Cu/Fe-HAO (PDB code: 4HVO), and Fe/'Cu'-HAO (PDB code: 4HVQ) showed that either metal can bind the active site, but Cu(II) is unable to bind the rubredoxin-like site. The crystal structure of HAO with a single metal ion exhibits a much higher average *B*-factor, which may explain why it is only 80% active. This work went on to show that PIC, a side product of metabolic pathways containing HAO, can remove the active site iron of HAO and reduce its activity. Furthermore, activity assays were used to demonstrate that the rubredoxin-like site is able to deliver Fe(II) to an empty HAO active site and restore catalytic activity.

Strategy for enriching O_2 at the active site

Another feature of the HAO active site is that upon bidentate coordination of 3-HAA to the ferrous ion, three hydrophobic loops move into a closed conformation (Figure 3).[24] While loops closing upon substrate binding is a common feature in enzymology, the hydrophobic nature of the residues moving toward the active site prompted a detailed study.[25] Asn27 and the backbone of Ile142 form a hydrogen bond only in the closed state, so they were chosen for analysis by site-directed mutagenesis. The kinetic parameters (k_{cat} and K_M) were determined for 3-HAA and O_2 with wild-type and several variants along with solving the X-ray crystal structures of ligand-bound forms. Asn27 and Ile142 variants were able to bind 3-HAA, but the loop movement observed in the wild-type enzyme was not found upon alteration of those residues. The K_M for O_2 was found to be 156 μM for wild-type HAO, and it drastically increased in the variants that are unable to form the 'closed' state that pulls hydrophobic residues toward the active site. The k_{cat} of those variants was also significantly reduced; however, it could be recovered if assays used an oxygen-saturated buffer to overcome the reduced oxygen affinity. These findings establish a mechanism by which an enzyme active site attracts and binds substrates with different chemical properties. The binding of the polar substrate, 3-HAA, to the charged active site induces structural changes that make the active site more hydrophobic to help attract the nonpolar substrate, O_2.

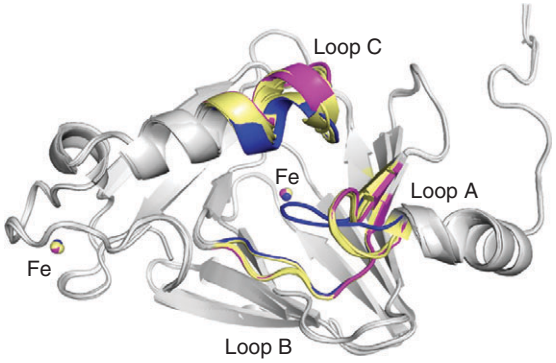

Figure 3 The crystal structure of the substrate-free enzyme is in a fully open form (gray, PDB code: 6VI5), whereas the structure of the bidentate complex is in a fully closed conformation with three hydrophobic loops moving to the iron center (blue, PDB code: 6VI7), increasing its hydrophobicity for attracting O_2 binding. The transient monodentate bound substrate (PDB code: 6VI6) and the oxygenated intermediates (PDB codes: 6VI8, 6VI9, 6VIA, 6X11, and 6VIB) exhibit a partially closed conformation (yellow and pink) Loop A: L20L21K22P23P24V25G26N27, Loop B: V40V41G42G43P45H46R47, and Loop C: I142V143T 144D145L146P147Pro148. The hydrophobic residues in the amino acid sequence. [Based on Yang *et al.*[25]]

CATALYTIC MECHANISM

In terms of the catalytic mechanism, HAO may be one of the best-understood dioxygenases due to extensive efforts to characterize numerous catalytic intermediates with X-ray crystallography.[35] Single crystals of HAO

Encyclopedia of Inorganic and Bioinorganic Chemistry, Online © 2011–2022 John Wiley & Sons, Ltd.

This article was published in the *Encyclopedia of Inorganic and Bioinorganic Chemistry* in 2022 by John Wiley & Sons, Ltd.
DOI: 10.1002/9781119951438.eibc2813

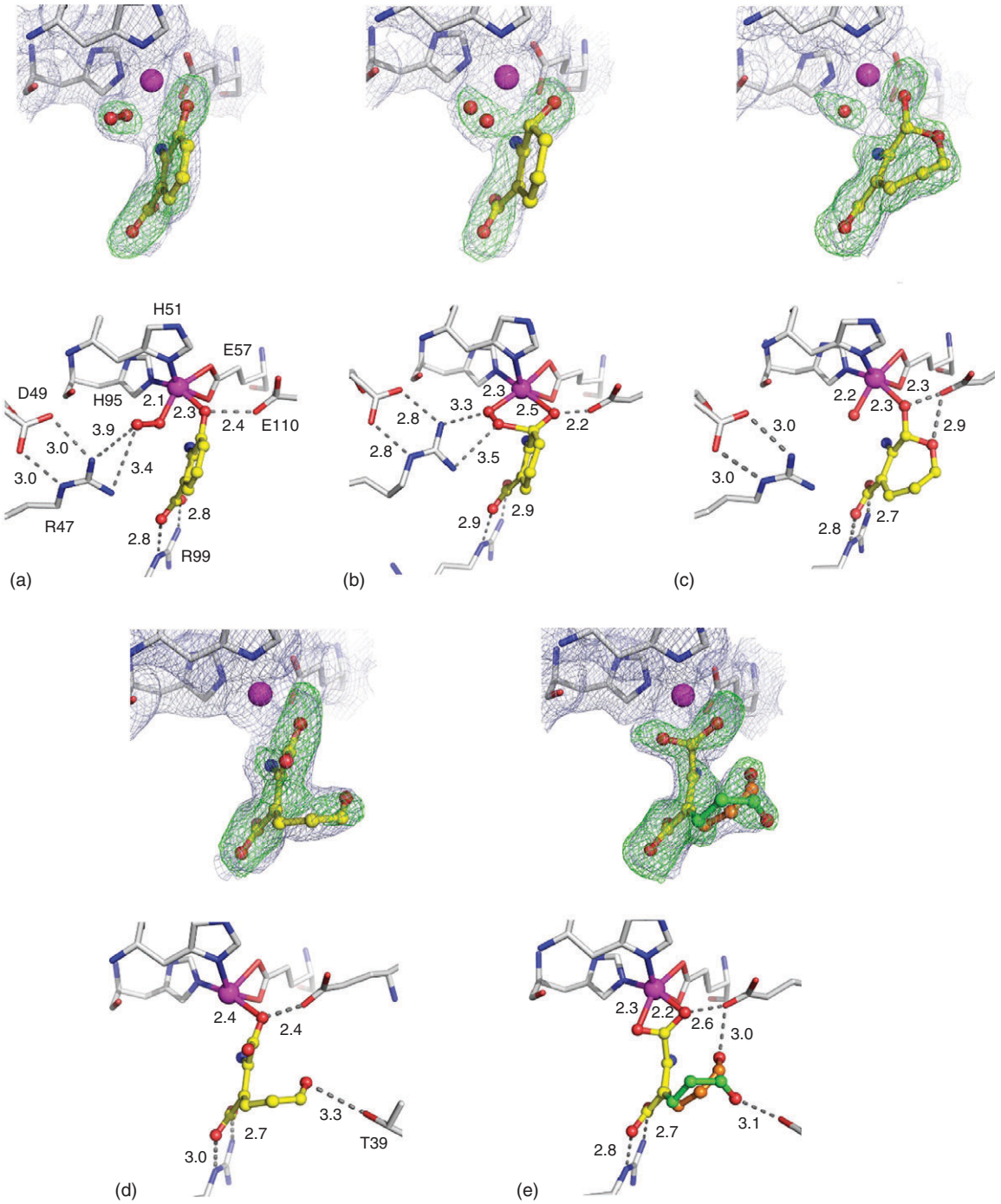

Figure 4 Catalytic pathway intermediates after O_2 binding to the enzyme-substrate complex: (a) the ternary complex (PDB code: 6VI8), (b) alkylperoxo intermediate (PDB code: 6VI9), (c) monooxygenated seven-membered lactone (PDB code: 6VI9), (d) initial dioxygenation product 3*E*,5*Z*,2*t*,4*c*-enol tautomer of ACMS (PDB code: 6X11), and (e) final dioxygenation product 3*E*,5*Z*,2*t*,4*t*-enol tautomer of ACMS (PDB code: 6VIB). The light blue $2F_{obs} - F_{calc}$ maps and green $F_{obs} - F_{calc}$ omit maps are contoured at 1.0 σ and 3.0 σ, respectively. Atom color code: gray, carbon (protein residues); yellow, carbon (ligand); blue, nitrogen; red, oxygen; magenta, iron. The bond lengths of the endogenous ligands are given in Table 1. The exogenous ligand to iron and H-bond network distances are labeled in the angstroms.

This article was published in the *Encyclopedia of Inorganic and Bioinorganic Chemistry* in 2022 by John Wiley & Sons, Ltd.
DOI: 10.1002/9781119951438.eibc2813

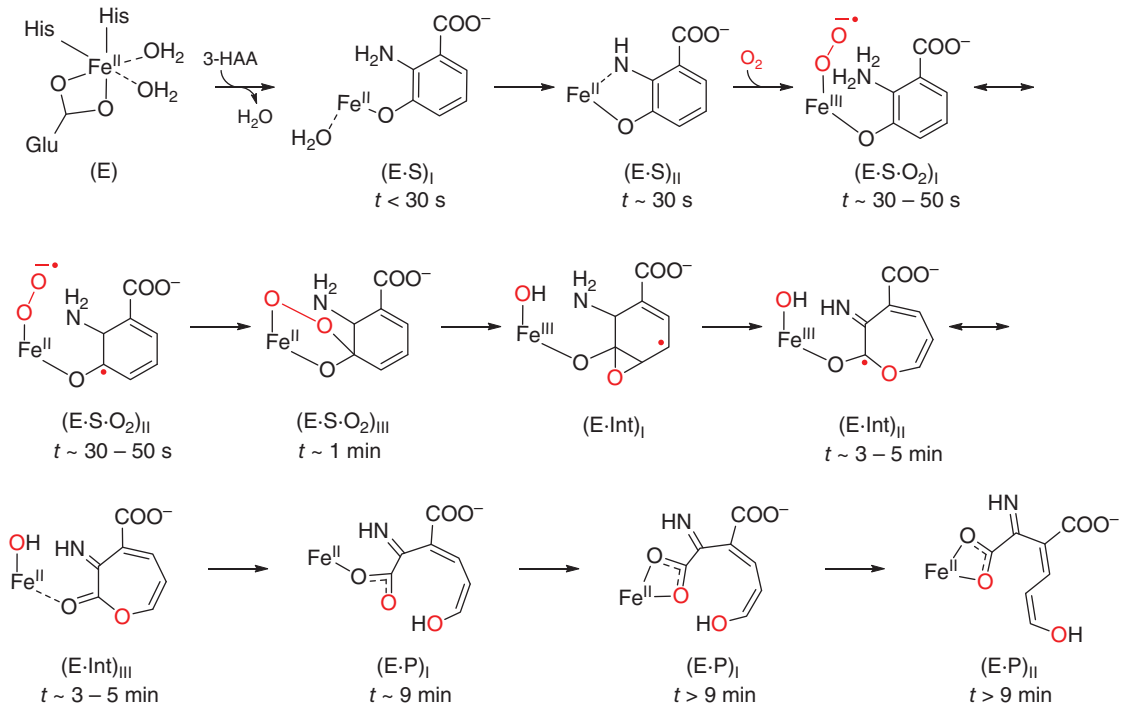

Figure 5 Proposed mechanism for the dioxygenation of 3-HAA as mediated by HAO. The *in crystallo* reaction times at which captured intermediates populate are given below their chemical structures. The abbreviations are enzyme (E), substrate (S), intermediate (Int), and product (P). [Based on Wang *et al.*[35]]

grown anaerobically before the addition of substrates are catalytically active, as shown by UV–vis spectroscopy, high-performance liquid chromatography, and high-resolution mass spectrometry.[35] Single crystal UV–vis and EPR spectroscopies indicated multiple intermediates during the reaction.[35] After screening thousands of crystals and collecting hundreds of data sets, two substrate-bound structures, the ternary complex with a ferric-superoxo, an alkylperoxo intermediate, an oxygenation intermediate with one oxygen atom inserted into the substrate phenyl ring, and two product structures were solved (Figure 4). These experimental observations give rise to a complete overview of the catalytic cycle shown in Figure 5.[35]

Three steps to bind two substrates

Crystals of HAO were grown anaerobically and soaked in mother liquor containing 3-HAA before flash cooling in liquid nitrogen. With this method, a monodentate 3-HAA-bound structure (PDB code: 6VI6) was captured prior to the normal bidentate binding mode (PDB code: 6VI7).[35] Interestingly, in the monodentate structure, the hydrophobic loop movement discussed above had not yet taken place.[35] If 3-HAA is allowed to soak for 30 s before quenching, the bidentate bound structure is observed with the loops in the closed conformation, priming the enzyme for oxygen binding.[25] ES complex crystals were soaked in oxygen-containing mother liquor various times before flash-cooling. Crystals anaerobically mixed with 3-HAA and flash-frozen 30–50 s after the introduction of oxygen showed the ternary complex (PDB code: 6VI8) with 3-HAA and O_2 both coordinated to the active site iron.[35]

Dioxygenation of 3-HAA

Quenching ES complex crystals after ~1 min of oxygen exposure gives an alkylperoxo structure (PDB code: 6VI9) with a nascent C—O bond between the distal oxygen atom of the iron-bound superoxide and 3-HAA. In both the ternary complex and the alkylperoxo structure, a second sphere arginine residue is observed to interact with the O_2 moiety, stabilizing and potentially directing the oxygen addition. Further incubation for 3–5 min with oxygen before quenching provides a monooxygenated seven-membered lactone intermediate (3D Structures, PDB code: 6VIA).[35] The distal oxygen atom from O_2 is now fully incorporated into the ring of 3-HAA in this intermediate structure. The capture of this intermediate demonstrates a stepwise oxygen insertion mechanism involving an O—O bond cleavage before both O-atoms are inserted into the substrate.

This article was published in the *Encyclopedia of Inorganic and Bioinorganic Chemistry* in 2022 by John Wiley & Sons, Ltd.
DOI: 10.1002/9781119951438.eibc2813

Product isomerization

After 9 min or more, the dioxygenation product, ACMS, is observed bound to the active site iron. Unlike the substrate, ACMS can exist in 32 potential conformations due to its double bonds and rotamers,[35] only one of which can nonenzymatically from QUIN. Earlier product-bound structures (PDB code: 6X11) have ACMS with monodentate coordination to the iron ion and the nascent aldehyde near to the imine, which is one single bond rotation from the QUIN forming conformer. At later times, the product bound structure (PDB code: 6VIB) transitions to ACMS bound in a bidentate mode, and the product aldehyde moiety is rotated away from the imine.[35] These conformational changes may be a way for HAO to direct the partitioning of metabolic flux toward enzymatic, energy-producing pathways and restrict QUIN formation.

ACKNOWLEDGEMENTS

This work was supported by the National Science Foundation grants CHE-1623856 and 1808637. Aimin Liu also acknowledges the support of the Lutcher Brown endowment fund.

RELATED ARTICLES

Nature of the Catecholate—Fe(III) Bond: High Affinity Binding and Substrate Activation in Bioinorganic Chemistry; Hydroxyquinol 1,2-Dioxygenase; 2,3-Dihydroxybiphenyl 1,2-Dioxygenase; Protocatechuate 3,4-Dioxygenase; Naphthalene 1,2-Dioxygenase; Iron Proteins with Mononuclear Active Sites; Mammalian Cysteine Dioxygenase

REFERENCES

1 BIOVIA, Discovery Studio Visualizer Software, Version 4.0, Dassault Systèmes, https://discover.3ds.com, San Diego, CA (2012).
2 AH Mehler, *J Biol Chem*, **218**, 241–54 (1956).
3 KL Colabroy and TP Begley, *J Am Chem Soc*, **127**, 840–1 (2005).
4 AH Bokman and BS Schweigert, *Arch Biochem Biophys*, **33**, 270–6 (1951).
5 HK Mitchell and JF Nyc, *Proc Natl Acad Sci U S A*, **34**, 1–5 (1948).
6 O Wiss, *Z. Naturforsch.*, **9b**, 740–1 (1954).
7 AH Mehler, *Science*, **145**, 817–9 (1964).
8 O Kurnasov, V Goral, KL Colabroy, S Gerdes, S Anantha, A Osterman and TP Begley, *Chem Biol*, **10**, 1195–204 (2003).
9 KL Colabroy and TP Begley, *J Bacteriol*, **187**, 7866–9 (2005).
10 Y Hasegawa, T Muraki, T Tokuyama, H Iwaki, M Tatsuno and PC Lau, *FEMS Microbiol Lett*, **190**, 185–90 (2000).
11 T Muraki, M Taki, Y Hasegawa, H Iwaki and PC Lau, *Appl Environ Microbiol*, **69**, 1564–72 (2003).
12 L Huo, F Liu, H Iwaki, T Li, Y Hasegawa and A Liu, *Proteins*, **83**, 178–87 (2015).
13 T Li, H Iwaki, R Fu, Y Hasegawa, H Zhang and A Liu, *Biochemistry*, **45**, 6628–34 (2006).
14 G Magni, M Di Stefano, G Orsomando, N Raffaelli and S Ruggieri, *Curr Med Chem*, **16**, 1372–90 (2009).
15 R Schwarcz, E Okuno, RJ White, ED Bird and WO Whetsell Jr, *Proc Natl Acad Sci U S A*, **85**, 4079–81 (1988).
16 MF Beal, NW Kowall, DW Ellison, MF Mazurek, KJ Swartz and JB Martin, *Nature*, **321**, 168–71 (1986).
17 TW Stone, *Pharmacol Rev*, **45**, 309–79 (1993).
18 R Schwarcz and R Pellicciari, *J Pharmacol Exp Ther*, **303**, 1–10 (2002).
19 Y Nishizuka, A Ichiyama, RK Gholson and O Hayaishi, *J Biol Chem*, **240**, 733–9 (1965).
20 F Liu, J Geng, RH Gumpper, A Barman, I Davis, A Ozarowski, D Hamelberg and A Liu, *J Biol Chem*, **290**, 15621–34 (2015).
21 RL Strausberg, EA Feingold, LH Grouse, JG Derge, RD Klausner, FS Collins, L Wagner, CM Shenmen, GD Schuler, SF Altschul, B Zeeberg, KH Buetow, CF Schaefer, NK Bhat, RF Hopkins, H Jordan, T Moore, SI Max, J Wang, F Hsieh, L Diatchenko, K Marusina, AA Farmer, GM Rubin, L Hong, M Stapleton, MB Soares, MF Bonaldo, TL Casavant, TE Scheetz, MJ Brownstein, TB Usdin, S Toshiyuki, P Carninci, C Prange, SS Raha, NA Loquellano, GJ Peters, RD Abramson, SJ Mullahy, SA Bosak, PJ McEwan, KJ McKernan, JA Malek, PH Gunaratne, S Richards, KC Worley, S Hale, AM Garcia, LJ Gay, SW Hulyk, DK Villalon, DM Muzny, EJ Sodergren, X Lu, RA Gibbs, J Fahey, E Helton, M Ketteman, A Madan, S Rodrigues, A Sanchez, M Whiting, A Madan, AC Young, Y Shevchenko, GG Bouffard, RW Blakesley, JW Touchman, ED Green, MC Dickson, AC Rodriguez, J Grimwood, J Schmutz, RM Myers, YS Butterfield, MI Krzywinski, U Skalska, DE Smailus, A Schnerch, JE Schein, SJ Jones, MA Marra and T Mammalian, *Proc Natl Acad Sci U S A*, **99**, 16899–903 (2002).
22 WA Koontz and R Shiman, *J Biol Chem*, **251**, 368–77 (1976).
23 D Nandi, ES Lightcap, YK Koo, X Lu, J Quancard and RB Silverman, *Int J Biochem Cell Biol*, **35**, 1085–97 (2003).
24 Y Zhang, KL Colabroy, TP Begley and SE Ealick, *Biochemistry*, **44**, 7632–43 (2005).
25 Y Yang, F Liu and A Liu, *J Biol Chem*, **293**, 10415–24 (2018).
26 CJ Parli, P Krieter and B Schmidt, *Arch Biochem Biophys*, **203**, 161–6 (1980).
27 MP Heyes, B Hutto and SP Markey, *Neurochem Int*, **13**, 405–8 (1988).
28 WP Todd, BK Carpenter and R Schwarcz, *Prep Biochem*, **19**, 155–65 (1989).
29 JL Walsh, WP Todd, BK Carpenter and R Schwarcz, *Adv Exp Med Biol*, **294**, 579–82 (1991).
30 JL Walsh, WP Todd, BK Carpenter and R Schwarcz, *Biochem Pharmacol*, **42**, 985–90 (1991).
31 KL Colabroy, H Zhai, T Li, Y Ge, Y Zhang, A Liu, SE Ealick, FW McLafferty and TP Begley, *Biochemistry*, **44**, 7623–31 (2005).

This article was published in the *Encyclopedia of Inorganic and Bioinorganic Chemistry* in 2022 by John Wiley & Sons, Ltd.
DOI: 10.1002/9781119951438.eibc2813

32 X Li, M Guo, J Fan, W Tang, D Wang, H Ge, H Rong, M Teng, L Niu, Q Liu and Q Hao, *Protein Sci*, **15**, 761–73 (2006).

33 I Dilovic, F Gliubich, G Malpeli, G Zanotti and D Matkovic-Calogovic, *Biopolymers*, **91**, 1189–95 (2009).

34 LS Pidugu, H Neu, TL Wong, E Pozharski, JL Molloy, SL Michel and EA Toth, *Acta Crystallogr D Struct Biol*, **73**, 340–8 (2017).

35 Y Wang, KF Liu, Y Yang, I Davis and A Liu, *Proc Natl Acad Sci U S A*, **117**, 19720–30 (2020).

This article was published in the *Encyclopedia of Inorganic and Bioinorganic Chemistry* in 2022 by John Wiley & Sons, Ltd.
DOI: 10.1002/9781119951438.eibc2813